Condition for alternans and stability of the 1:1 response pattern in a "memory" model of paced cardiac dynamics

E. G. Tolkacheva,[1] D. G. Schaeffer,[2] Daniel J. Gauthier,[1,3] and W. Krassowska[3]
[1]*Department of Physics, Duke University, Box 90305, Durham, North Carolina 27708*
[2]*Department of Mathematics, Duke University, Box 90305, Durham, North Carolina 27708*
[3]*Department of Biomedical Engineering, and Center for Nonlinear and Complex Systems, Duke University, Durham, North Carolina 27708*
(Received 21 October 2002; published 12 March 2003)

We analyze a mathematical model of paced cardiac muscle consisting of a map relating the duration of an action potential to the preceding diastolic interval as well as the preceding action potential duration, thereby containing some degree of "memory." The model displays rate-dependent restitution so that the dynamic and S1-S2 restitution curves are different, a manifestation of memory in the model. We derive a criterion for the stability of the 1:1 response pattern displayed by this model. It is found that the stability criterion depends on the slope of both the dynamic and S1-S2 restitution curves, and that the pattern can be stable even when the individual slopes are greater or less than one. We discuss the relation between the stability criterion and the slope of the constant-BCL restitution curve. The criterion can also be used to determine the bifurcation from the 1:1 response pattern to alternans. We demonstrate that the criterion can be evaluated readily in experiments using a simple pacing protocol, thus establishing a method for determining whether actual myocardium is accurately described by such a mapping model. We illustrate our results by considering a specific map recently derived from a three-current membrane model and find that the stability of the 1:1 pattern is accurately described by our criterion. In addition, a numerical experiment is performed using the three-current model to illustrate the application of the pacing protocol and the evaluation of the criterion.

DOI: 10.1103/PhysRevE.67.031904 PACS number(s): 87.19.Hh, 05.45.−a, 87.10.+e

I. INTRODUCTION

Several experimental and modeling studies have suggested that an abnormal cardiac rhythm known as action potential duration (APD) alternans is a first stage in the development of ventricular arrhythmias [1,2], which often lead to sudden cardiac death. APD alternans can be induced by pacing cardiac tissue at a rapid rate, and it is characterized by short-long alternations of the durations of subsequent action potentials. The transition from the 1:1 response, in which every stimulus elicits an action potential and all APDs are the same, to alternans (2:2 response) is believed to be determined by the restitution properties of the cardiac membrane. Specifically, to predict the pacing rates at which the 1:1 response is stable, one needs to construct the restitution curve (RC) by plotting APD as a function of the preceding diastolic interval (DI). Nolasco and Dahlen [3] proposed that the 1:1 response is stable when the slope of the RC is less than one, based on related ideas that were outlined nearly a century ago [4].

Placing their work on a firm mathematical foundation, Guevara *et al.* [5] proposed to model the response of cardiac tissue to pacing by an equation of the form

$$A_{n+1}=f(D_n), \tag{1}$$

where f is the RC, and the APD on the $n+1$th pace is denoted by A_{n+1} and the preceding DI by D_n. The APD and DI are related through the pacing relation

$$A_n+D_n=B, \tag{2}$$

where B is the pacing interval. By inserting Eq. (2) into Eq. (1), it is seen that the dynamics is governed by a one-dimensional map given by

$$A_{n+1}=f(B-A_n). \tag{3}$$

Guevara *et al.* showed that the 1:1 response pattern is stable when the slope of the RC is less than one; that is, when

$$\left|\frac{df}{dA_n}\right|_{A_n=A^*}=\left|\frac{df}{dD_n}\right|\leqslant 1, \tag{4}$$

where $A^*=f(B-A^*)$ is the fixed point of the map.

However, criterion (4) often fails in an experimental setting. For example, Gilmour and collaborators [6,7] have shown that the 1:1 pattern can be unstable and replaced by APD alternans even when the slope of the RC less than one. These observations suggest that the dynamics of paced cardiac tissue cannot be described by the one-dimensional mapping (3).

Another experimental observation that points to the shortcoming of the model is that the RC depends on the method by which it is measured. The RC is often measured using the *S1-S2 protocol* in which a premature stimulus "S2" is delivered at an interval $B_{S_1S_2}$ after pacing the tissue with a sufficiently large number of "S1" stimuli at a pacing interval B_{S_1}, so that the tissue reaches equilibrium and produces action potential with duration A_{S_1}. The S1-S2 RC is determined by measuring the resulting APD, denoted by $A_{S_1S_2}$, for various coupling intervals $B_{S_1S_2}$, and visualized by plotting $A_{S_1S_2}$ as a function of $D_{S_1S_2}=B_{S_1S_2}-A_{S_1}$. Experimental

 ©2003 The American Physical Society

studies [8–10] have shown that this RC depends on the choice of B_{S_1}; that is, the model displays rate-dependent restitution. In contrast, an analysis of map (3) shows that the predicted S1-S2 RCs are identical for all B_{S_1}.

Based on a series of experiments using dog hearts, Gilmour and collaborators [11,12] proposed that the 1:1 pattern becomes unstable when the slope of the RC determined by the *dynamic protocol* is greater than one. In this protocol, the pacing interval is held fixed until the tissue reaches equilibrium, and then progressively shortened, yielding pairs of values (A^*, D^*) for each B_{S_1}. Experimental studies have shown that the S1-S2 and dynamic RCs differ significantly, and that the slope of the S1-S2 RC can be either shallower [11] or steeper [8] than the slope of the dynamic RC. Note that this is in contrast to the predictions of the one-dimensional map (3), for which the dynamic and S1-S2 RCs are identical. Unfortunately, it appears that the criterion proposed by Gilmour and collaborators does not apply to all situations: Recent experiments with frogs [13] and numerical modeling studies of a canine ventricular model [14] have shown that a stable 1:1 response can be observed when the slope of the dynamic RC is greater than one.

These considerations indicate the need for investigating new models that display rate-dependent restitution, but are simple enough so that the analysis of the models can lead to the development of a new criterion for the stability of the 1:1 response pattern and the bifurcation to alternans. A simple model with this property of the form

$$A_{n+1}=F(A_n,D_n) \tag{5}$$

was proposed on an empirical basis by Otani and Gilmour [7]. Using pacing relation (2), it is seen that this model is still represented by a one-dimensional mapping given by

$$A_{n+1}=F(A_n,B-A_n). \tag{6}$$

However, as discussed below, the explicit dependence of F on both A_n and D_n endows the model with memory so that it displays rate-dependent restitution and the S1-S2 and dynamic RCs differ [7]. We note that a mapping of this form was derived analytically [15] from a three-ionic-current membrane model [16].

The primary purpose of this paper is to derive a criterion for the stability of the 1:1 response pattern and the transition to alternans for the map (6) *in terms of readily measured quantities*, i.e., the slope $S_{S_1S_2}$ of the S1-S2 RC and the slope S_{dyn} of the dynamic RC. In addition, we discuss the relation between the stability criterion and the slope S_{BCL} of an RC introduced by Otani and Gilmour [7] (the so called constant-BCL RC) describing the transient response of the tissue as it relaxes to its equilibrium value. The paper is organized in the following way. In Sec. II, we illustrate graphically the difference between dynamic, S1-S2, and constant-BCL RCs for map (6). Section III presents the derivation of a new stability criterion from the map, and Sec. IV describes a protocol for evaluating the criterion from experimental measurements. Sections V and VI demonstrate the accuracy of the new criterion by applying it to the mapping model of cardiac dynamics derived in Ref. [15] and to a three-current model of cardiac membrane [16], respectively. Finally, Sec. VII discusses the advantages and limitations of the proposed stability criterion.

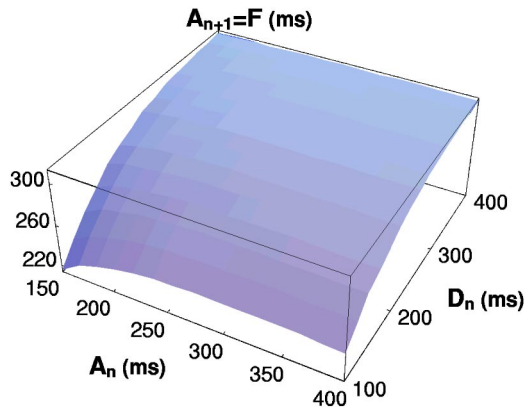

FIG. 1. An illustration of the function F representing cardiac restitution.

II. GRAPHICAL ILLUSTRATION OF THE DYNAMIC, S1-S2, AND CONSTANT-BCL RESTITUTION CURVES

The origin of rate-dependent restitution can be illustrated graphically by taking A_n and D_n as independent variables and plotting F as a two-dimensional surface, as shown in Fig. 1 for the map derived from the three-current model (described in Sec. V). Note that the discussions in this and the following sections are entirely general unless noted otherwise, and that we use a specific form of F for illustrative purposes only. If the surface is constant as a function of A_n, the model shows no rate-dependent restitution and the dynamic, S1-S2, and constant-BCL RCs are identical. For typical models of cardiac muscle, the function F tends to display the strongest dependence on A_n when A_n is short, as in the case for the model used to generate the surface in Fig. 1.

A. Dynamic restitution curve

In the context of the mapping (6), the dynamic RC can be given the following mathematical interpretation. Consider the case when the tissue paced at a constant B to produce a 1:1 response and for a long enough time so that the dynamics settle down to the steady-state value A^* (the fixed point). Under this condition [17]

$$A_{n+1}=A_n\equiv A^*, \tag{7}$$

and the corresponding DI is

$$D^*=B-A^*. \tag{8}$$

Inserting Eqs. (7) and (8) into (6), the fixed point can be found from the solution to

$$A^*=F(A^*,B-A^*)=F(A^*,D^*). \tag{9}$$

The set of fixed points A^* and the associated diastolic intervals D^*, recorded for different Bs, is the dynamic RC.

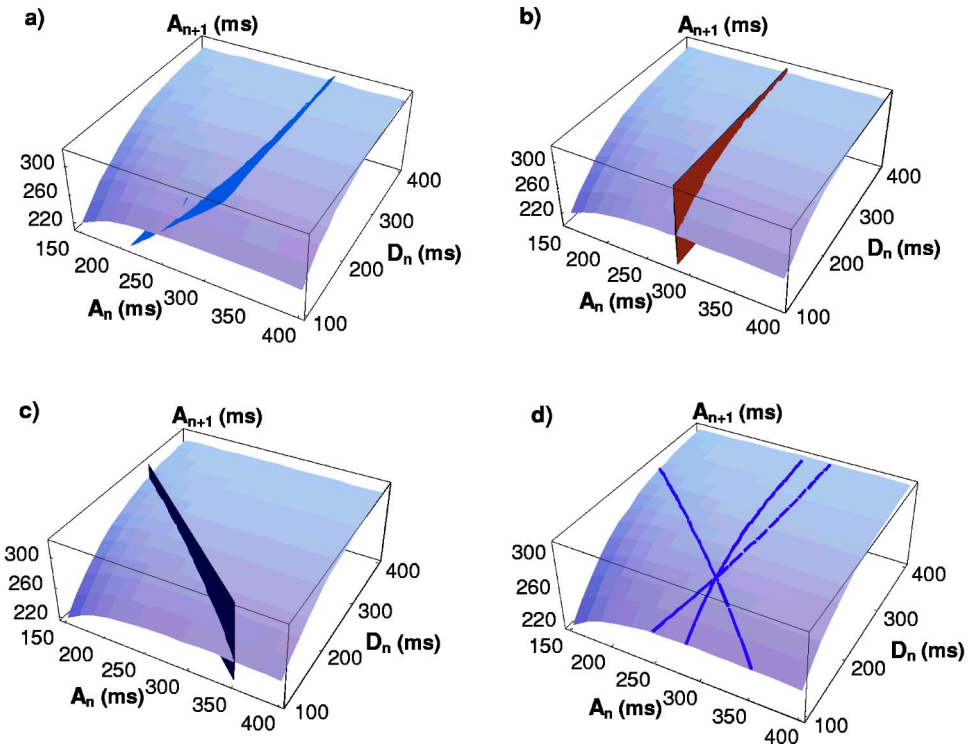

FIG. 2. Graphical illustration of the (a) dynamic, (b) S1-S2, (c) constant-BCL RCs, and (d) their intersection at a fixed point of the map for $B=450$ ms. The dynamic RC is the intersection of surfaces $A_{n+1}=F(A_n,D_n)$ and $A_{n+1}=A_n$. The S1-S2 RC is the intersection of surfaces $A_{n+1}=F(A_n,D_n)$ and $A_n=A^*_{S_1}=$const. The constant-BCL RC is the intersection of the function F with surface $B=$const.

Graphically, this curve is shown in Fig. 2(a) as the intersection of the surfaces described by Eq. (5) and left part of Eq. (7): $A_{n+1}=A_n$. Therefore, we see that the dynamic protocol samples only a very limited region of the two-dimensional surface F because of the constraint imposed by Eq. (9). We can see from the graph that the value of A^* is almost constant for long DIs, since this specific choice of the restitution function F is nearly constant at this region.

In experiments, the dynamic RC is plotted in two dimensions as pairs of points (A^*, D^*), as shown in Fig. 3 (solid lines). This plot is a projection of the three-dimensional RC shown in Fig. 2(a) onto the $A_{n+1}-D_n$ plane. For a given set of model parameters, there exists only a single, unique dynamic RC.

B. S1-S2 restitution curve

Following the above description of the S1-S2 protocol, the S1-S2 RC can be obtained by noting that all APDs preceding the S2 stimulus are equal, so that

$$A_n \equiv A^*_{S_1} = \text{const}, \tag{10}$$

where $A^*_{S_1}$ is the steady-state APD at the pacing interval B_{S_1}. The APD $A_{S_1S_2}$ can be determined as

$$A_{S_1S_2}=F(A^*_{S_1},D_{S_1S_2})=F(A^*_{S_1},B_{S_1S_2}-A^*_{S_1}). \tag{11}$$

Thus, according to Eq. (11), the S1-S2 RC is the intersection of surface (5) with the vertical plane defined by Eq. (10) (for a given value of B_{S_1}). Figure 2(b) shows example of S1-S2 RC for the given value of $A^*_{S_1}$. Note that a single surface defined by Eq. (10) may correspond to two or more values of B_{S_1} for a more complicated function F than that shown in Fig. 2.

Comparing Figs. 2(a) and 2(b) for large values of the DI, we see that the S1-S2 RCs are nearly parallel to the dynamic

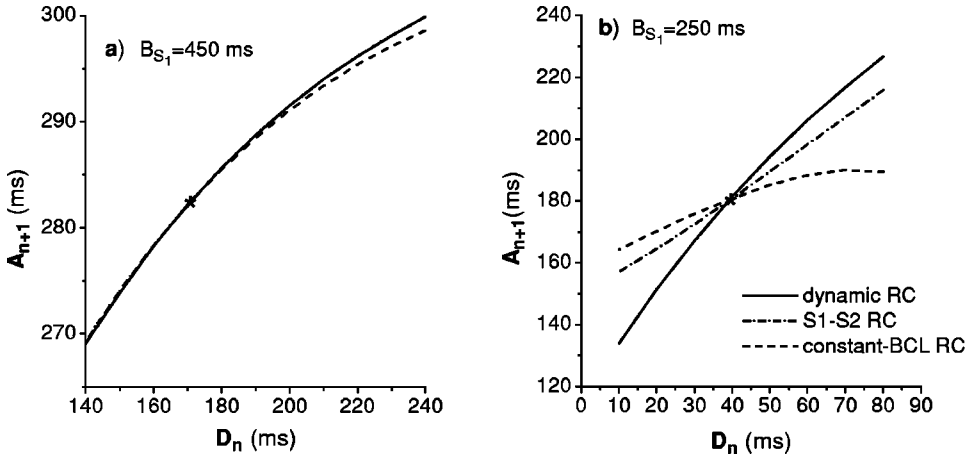

FIG. 3. A projection of Fig. 2(d) on the $A_{n+1}-D_n$ plane indicating the intersection of the dynamic RC (solid line), S1-S2 RC (dot-dashed line), and constant-BCL RC (dashed line) for different S1-S1 pacing rates of (a) $B_{S_1}=450$ ms and (b) $B_{S_1}=250$ ms. Stars represent intersection points. Note that the S1-S2 RC is indistinguishable from the dynamic RC in (a).

RC and all of them have essentially the same APD values, because this specific form of the function F is nearly flat in this region.

C. Constant-BCL restitution curve

A third RC introduced by Otani and Gilmour, but not discussed as often in the literature, describes the transient response of paced cardiac tissue for constant BCL, as it approaches the equilibrium value following a change in BCL. In this situation, A_n and D_n are related through Eq. (2), so that the transient dynamics are given by the intersection of F and the vertical plane defined by Eq. (2), as shown in Fig. 2(c) for the case of $B=450$ ms. We call this as a constant-BCL RC (following Ref. [7]), because it contains all values of A_n and D_n, both transients and steady state recorded for a constant BCL.

D. Intersection of the dynamic, S1-S2, and constant-BCL restitution curves

The point where the dynamic RC, a constant-BCL RC, and a S1-S2 RC intersect play an important role in determining the stability of the 1:1 response pattern at that point. Graphically, for a given point on the dynamic RC [one point along the intersection of F and the plane defined by $A_n = A_{n+1}$ as shown in Fig. 2(a)], there exists a single vertical plane defined by $A_n = A^*_{S_1}$ that also passes through this point. At this simultaneous intersection point

$$A^* = A_{S_1} = A_{S_1S_2}, \quad D^* = D_{S_1} = D_{S_1S_2},$$

and

$$B = B_{S_1} = B_{S_1S_2}. \tag{12}$$

For the given value of $B = B_{S_1} = B_{S_1S_2}$, there is also a single constant-BCL curve passing through this intersection point. The intersection of all three RCs is presented graphically in Fig. 2(d) for $B=450$ ms.

A projection of the curves shown in Fig. 2(d) onto the $A_{n+1}-D_n$ plane showing the intersection of three RCs is presented in Fig. 3 for two different values of pacing interval B. As can be seen from the figure, the local S1-S2, constant-BCL, and dynamic RCs are nearly identical for the relatively large BCL ($B=450$ ms) and differ substantially (with different slopes at the intersection point) for smaller value of BCL ($B=200$ ms). (The fact that $S_{dyn} > S_{S_1S_2}$ is specific to our choice of F; in principle, other functions could result in the slopes being the same or $S_{dyn} < S_{S_1S_2}$.) The immediate response of the tissue to an abrupt change in B is determined by the original S1-S2 RC, but in the long term, the APD settles down to a new point on the dynamic RC. Hence, all transient response after an abrupt change in B occurs along the constant-BCL RC. As will be shown in the following section, the stability of the 1:1 response pattern must incorporate information about the detailed shape of the surface F at the intersection point, and neither the slope of the dynamic nor the S1-S2 curve alone does so.

III. STABILITY CRITERION FOR THE 1:1 PATTERN AND THE BIFURCATION TO ALTERNANS

The problem of determining the stability of the 1:1 response to periodic pacing is equivalent to determining the stability of the fixed point A^* of the one-dimensional map (6). As described in Ref. [17], the stability of the fixed point is determined from

$$\left.\frac{dF}{dA_n}\right|_{A_n=A^*} = \left.\left(\frac{\partial F}{\partial A_n}\frac{dA_n}{dA_n} + \frac{\partial F}{\partial D_n}\frac{dD_n}{dA_n}\right)\right|_{A_n=A^*} \equiv F'. \tag{13}$$

Realizing that $dA_n/dA_n = 1$ and $dD_n/dA_n = -1$ [using pacing relation (2)], Eq. (13) can be written as

$$F' = \left.\frac{\partial F}{\partial A_n}\right|_{A_n=A^*} - \left.\frac{\partial F}{\partial D_n}\right|_{A_n=A^*}. \tag{14}$$

The fixed point is stable if $|F'|<1$ and unstable if $|F'|>1$. When $|F'|\geqslant 1$, the existence of a 2:2 response (alternans) becomes possible. The derivative given in Eq. (14) and the stability criterion are not new; Otani and Gilmour [7] previously presented the same result. However, it is not obvious how to measure F' or the partial derivatives in Eq. (14) experimentally. The primary purpose of this paper is to show how these derivatives can be obtained and the criterion evaluated from a minor modification of a standard experimental protocol.

There are two ways of evaluating F' experimentally. First, note that F' describes the response of the tissue when it is perturbed away from its equilibrium value A^* for constant model parameters, including the pacing rate B. Hence, in mathematical terms, $-F'$ is the slope S_{BCL} of the constant-BCL RC evaluated at the fixed point. [The minus sign comes from the fact that the slope of RC is the derivative of the function F with respect to D_n whereas formula (14) is evaluated with respect to A_n.]

A second way of determining F' is to express the partial derivatives in terms of the slopes of dynamic and S1-S2 RCs. Note that the slope of the dynamic RC is given by

$$S_{dyn} \equiv \frac{\partial A^*}{\partial D^*} = \frac{\partial F}{\partial A^*}\frac{\partial A^*}{\partial D^*} + \frac{\partial F}{\partial D^*}\frac{\partial D^*}{\partial D^*}, \tag{15}$$

where the last expression results from differentiating Eq. (9) for the dynamic RC. Realizing that $\partial D^*/\partial D^* = 1$ and $\partial F/\partial A^* = \partial F/\partial A_n|_{A_n=A^*}$, since both represent the partial derivative of F with respect to its first argument evaluated at the fixed point, we find that

$$S_{dyn} = \frac{\partial F/\partial D_n|_{A_n=A^*}}{1-\partial F/\partial A_n|_{A_n=A^*}}. \tag{16}$$

Next, note that the slope of the S1-S2 RC that intersects the dynamic RC at the fixed point for a given B (see Sec. II A) is given by [differentiating Eq. (11) for the S1-S2 RC]

$$S_{S_1S_2} \equiv \left.\frac{\partial A_{S_1S_2}}{\partial D_{S_1S_2}}\right|_{B_{S_1}=B_{S_1S_2}=B} = \left.\left(\frac{\partial F}{\partial A^*_{S_1}}\frac{\partial A^*_{S_1}}{\partial D_{S_1S_2}} + \frac{\partial F}{\partial D_{S_1S_2}}\frac{\partial D_{S_1S_2}}{\partial D_{S_1S_2}}\right)\right|_{B_{S_1}=B_{S_1S_2}=B}. \tag{17}$$

Using the facts that $\partial A^*_{S_1}/\partial D_{S_1S_2}=0$ and $\partial D_{S_1S_2}/\partial D_{S_1S_2}=1$, we find that

$$S_{S_1S_2} = \left.\frac{\partial F}{\partial D_{S_1S_2}}\right|_{B_{S_1}=B_{S_1S_2}=B} = \left.\frac{\partial F}{\partial D_n}\right|_{A_n=A^*}, \tag{18}$$

where the later equality results from the observation that both derivatives represent the partial derivative of F with respect to its second argument evaluated at the fixed point.

Using Eqs. (14), (16), and (18), the stability criterion for the stability of the fixed point A^* of map (6), and hence of the stability of the 1:1 response pattern, is given by

$$|F'| = |S_{\mathrm{BCL}}| = \left|1 - \left(1 + \frac{1}{S_{dyn}}\right) S_{S_1S_2}\right| < 1. \tag{19}$$

Equation (19) is the primary result of this paper, giving a prescription for relating readily measured quantities to the stability of the 1:1 response pattern. It involves either the slope of the constant-BCL RC or the slope of both the dynamic and S1-S2 RCs calculated at their intersection point. Thus, the existence of alternans (when $|F'| \geqslant 1$) is determined by the combination of S_{dyn} and $S_{S_1S_2}$ and not by either of the slopes individually.

IV. NEW PACING PROTOCOL

Since there exists an infinite number of constant-BCL and S1-S2 RCs, it might appear that the experimental or computational effort in determining the slopes in criterion (19) would make our proposal impractical. However, the slope of the constant-BCL or the S1-S2 RCs is only needed at the intersection point with the dynamic RC for a given value of B, and hence the knowledge of the full surface F is not needed to determine the stability of the fixed point. To reduce the experimental or computational effort, we suggest a *modified dynamic protocol* that allows one to measure S_{dyn}, $S_{S_1S_2}$, and S_{BCL} at the each fixed point with minimal effort:

(1) Choose a value of $B=B_i$ (initially, B should be relatively long), wait until the APD achieves steady state, and measure its value A^*_i. This value will be used to construct the dynamic RC and compute S_{dyn} [see step (9)].

(2) Adjust the pacing interval to a new value B_{long} for a single pace, and measure the ensuing APD (denoted by A_{long}). B_{long} must be sufficiently large so that the difference between A_{long} and A^*_i is above measurement error, but small enough so that it falls within an approximate linear neighborhood of the fixed point. Values of $B_{long}-B$ of the order of a few tens of milliseconds should suffice for typical cardiac tissue.

(3) Return the pacing interval to B, and measure all APDs until the tissue returns to its equilibrium value A^*_i. These transient values A^{trans}_i are used to determine S_{BCL} [see step (7)].

(4) Adjust the pacing interval to a new value B_{short} for a single pace, and measure the ensuing APD (denoted by A_{short}).

(5) Repeat step (3).

(6) Use A_{long} and A_{short} to evaluate $S_{S_1S_2}$ at the fixed point A^*_i based on the central difference formula for estimating a derivative:

$$S_{S_1S_2} \approx \frac{A_{long}-A_{short}}{B_{long}-B_{short}}. \tag{20}$$

Here we used the fact that $B_{long}-B_{short}=D_{long}-D_{short}$ for the S1-S2 RC.

(7) Apply a linear least-squares fitting method [18] to fit all transient points A^{trans}_i in order to determine S_{BCL} at the fixed point A^*_i.

(8) Repeat steps (1)–(7) for several values of BCL in equal intervals $B_{i+1}=B_i-\Delta B$, where ΔB should be of the order of tens of milliseconds.

(9) Determine S_{dyn} at the fixed point A^*_i using central difference approximation [19,20]

$$S_{dyn} \approx \frac{A^*_{i-1}-A^*_{i+1}}{D^*_{i-1}-D^*_{i+1}}. \tag{21}$$

This protocol requires little additional work in comparison to measuring the dynamic RC. We note that steps 2–7 can be repeated to reduce the random errors occurring in experimental measurements.

V. EXAMPLE: APPLYING THE STABILITY CRITERION TO A MAP

In this section we apply stability criterion (19) to the map derived in Ref. [15] from the three-current model of cardiac membrane developed by Fenton and Karma [16]. Since the three-current model used here employs different notation than the original one, the Appendix provides a short summary of the model and lists the parameter values. Under an approximation that the parameter κ of the three-current model is large, the restitution function F has an explicit form

$$F(\tilde{A}_n,\tilde{D}_n) = \left\{ C_1 - \frac{r_{cur}}{P(\tilde{A}_n,\tilde{D}_n)} + \sqrt{1 - \frac{C_2}{P(\tilde{A}_n,\tilde{D}_n)} + \left[\frac{r_{cur}}{P(\tilde{A}_n,\tilde{D}_n)}\right]^2}\right\}, \tag{22}$$

where

TABLE I. Typical parameter values for the three-current ionic model.

Parameter (three-current model)	Value (ms)	Parameter	Value (dim'less)
τ_{sclose}	1000	V_{crit}	0.13
τ_{slow}	127	V_{sig}	0.85
τ_{ung}	130	κ	40
τ_{sopen}	80	V_{out}	0.1
τ_{fopen}	18		
τ_{fclose}	10		
τ_{fast}	0.25		

$$P(\tilde{A}_n,\tilde{D}_n)=1-[1-G(\tilde{A}_n)e^{-\tilde{A}_n}]e^{-\tilde{D}_n r_{gate}}, \quad (23)$$

$$G(\tilde{A}_n)=\frac{r_{cur}\tilde{A}_n-(1-V_{crit})r_{mix}}{1-\exp[-\tilde{A}_n+r_{mix}(V_{sig}-V_{crit})/r_{cur}]}, \quad (24)$$

$\tilde{A}_n$ and $\tilde{D}_n$ are dimensionless variables given by

$$\tilde{A}_n=\frac{A_n}{\tau_{sclose}}, \quad \tilde{D}_n=\frac{D_n}{\tau_{sclose}}, \quad (25)$$

and the constants C_1 and C_2 are

$$C_1=1+\frac{r_{mix}}{r_{cur}}(V_{sig}-V_{crit}), \quad C_2=2[r_{cur}+r_{mix}(V_{sig}-1)]. \quad (26)$$

The remaining constants are ratios of the time constants of the three-current model as

$$r_{gate}=\frac{\tau_{sclose}}{\tau_{sopen}}, \quad r_{cur}=\frac{\tau_{slow}}{\tau_{ung}}, \quad r_{mix}=\frac{\tau_{slow}}{\tau_{sclose}}. \quad (27)$$

Values of these time constants, as well as V_{sig} and V_{crit}, are given in Table I.

Since the map (22)–(24) has an explicit form, we can determine the derivatives at the fixed point $\tilde{A}^*$ using expressions

$$\left.\frac{\partial F}{\partial \tilde{A}_n}\right|_{\tilde{A}_n=\tilde{A}^*}=\left.\frac{\partial F}{\partial P}\frac{\partial P}{\partial \tilde{A}_n}\right|_{\tilde{A}_n=\tilde{A}^*},$$

$$\left.\frac{\partial F}{\partial \tilde{D}_n}\right|_{\tilde{A}_n=\tilde{A}^*}=\left.\frac{\partial F}{\partial P}\frac{\partial P}{\partial \tilde{D}_n}\right|_{\tilde{A}_n=\tilde{A}^*}, \quad (28)$$

where

$$\left.\frac{\partial F}{\partial P}\right|_{\tilde{A}_n=\tilde{A}^*}=\frac{1}{(P^*)^2}\left[r_{cur}+\frac{C_2-2r_{cur}^2/P^*}{2\sqrt{1-C_2/P^*+(r_{cur}/P^*)^2}}\right], \quad (29)$$

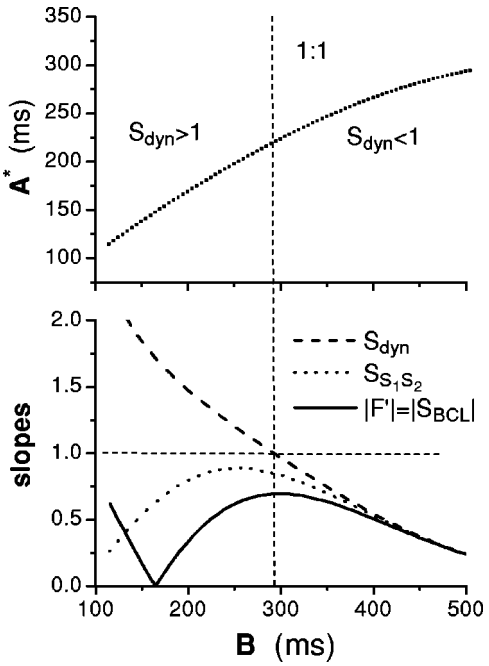

FIG. 4. (a) The bifurcation diagram and (b) slopes S_{dyn}, $S_{S_1S_2}$, and $|F'|$ (which is equal to S_{BCL} by definition) plotted as functions of BCL. Parameter values from Table I are used. The dashed vertical line indicates the BCL, where $S_{dyn}=1$.

$$\left.\frac{\partial P}{\partial \tilde{A}_n}\right|_{\tilde{A}_n=\tilde{A}^*}=\exp(-r_{gate}^*\tilde{D}^*-\tilde{A}^*)\left(\left.\frac{\partial G}{\partial \tilde{A}_n}\right|_{\tilde{A}_n=\tilde{A}^*}-G^*\right), \quad (30)$$

$$\left.\frac{\partial P}{\partial \tilde{D}_n}\right|_{\tilde{A}_n=\tilde{A}^*}=r_{gate}\exp(-r_{gate}\tilde{D}^*)[1-G^*\exp(-\tilde{A}^*)], \quad (31)$$

$$\left.\frac{\partial G}{\partial \tilde{A}_n}\right|_{\tilde{A}_n=\tilde{A}^*}=\frac{r_{cur}-G^*\exp[-\tilde{A}^*+r_{mix}(V_{sig}-V_{crit})/r_{cur}]}{1-\exp[-\tilde{A}^*+r_{mix}(V_{sig}-V_{crit})/r_{cur}]}, \quad (32)$$

and

$$P^*\equiv P(\tilde{A}^*,\tilde{D}^*), \quad G^*\equiv G(\tilde{A}^*). \quad (33)$$

Using Eqs. (28)–(32) and combining them according to Eqs. (16) and (18), we find S_{dyn} and $S_{S_1S_2}$, and from Eq. (14) we determine $|F'|$ at the fixed point of the map. Figure 4 shows the A^* and the derivatives as a function of B, obtained using the ''standard'' parameter values given in Table I, for which the model does not exhibit alternans. As can be seen from the graph, a stable 1:1 response occurs for Bs below $\sim$300 ms, where $S_{dyn}>1$ (indicated by the dashed vertical line). Figure 4(b) demonstrates that $S_{S_1S_2}$ and $|F'|$ are below one for the entire range of B's.

Figure 5 shows the results obtained with parameter values, for which the model exhibits alternans (τ_{sopen} is adjusted from 80 ms to 50 ms). Figure 5(a) shows that altern-

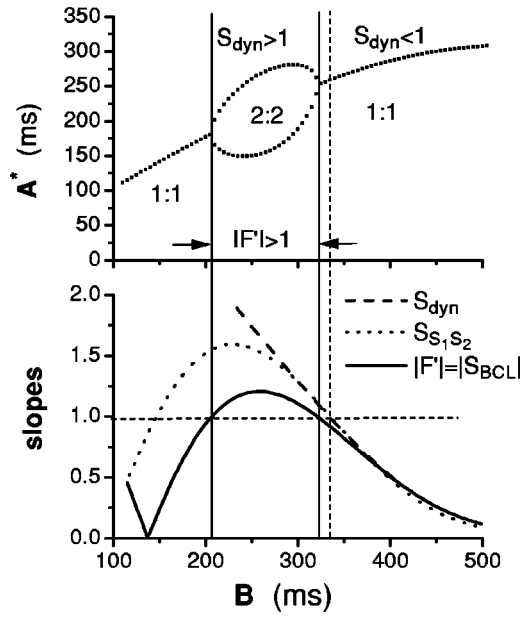

FIG. 5. (a) The bifurcation diagram and (b) derivatives S_{dyn}, $S_{S_1S_2}$, and $|F'|$ (which is equal to S_{BCL} by definition) plotted as functions of BCL. Parameter values from Table I were used, except $\tau_{sopen}=50$ ms. The dashed vertical line indicates the BCL, where $S_{dyn}=1$.

ans occur only in the region between the two solid vertical lines where $|F'|>1$, as can be seen in Fig. 5(b). To the left of the dashed line, where $S_{dyn}>1$, both a 1:1 response or alternans are seen. Thus, alternans indeed occurs in the range of Bs for which $|F'|>1$, while neither S_{dyn} nor $S_{S_1S_2}$ determines whether alternans exist or not. Note that both S_{dyn} and $S_{S_1S_2}$ are greater than one for 150 ms$\lesssim B\lesssim$200 ms, where $|F'|<1$ and the 1:1 response is stable.

VI. EXAMPLE: APPLYING THE STABILITY CRITERION TO AN IONIC MODEL

To illustrate how to apply the modified dynamic protocol described in Sec. IV to determine the response of the 1:1 response pattern, we perform a numerical experiment using the three-current model described in the Appendix. The ordinary differential equations of the model, (A1), (A4), and (A8), are integrated using Gear's backward differentiation method with a variable step size no larger than 0.1 ms. The APD was computed as a time interval during which the voltage $v>V_{crit}$. To assure that the steady state is reached, at least 1000 stimuli are applied.

Figure 6 presents results obtained by applying this procedure. The left panel of Fig. 6 presents the dynamic and local S1-S2 RCs. The dynamic RC is obtained using step 1 of the modified dynamic protocol discussed in Sec. IV and consists of pairs of points (A^*,D^*). Points A, B, C, D indicate fixed points of the response (i.e., the steady-state values) for four

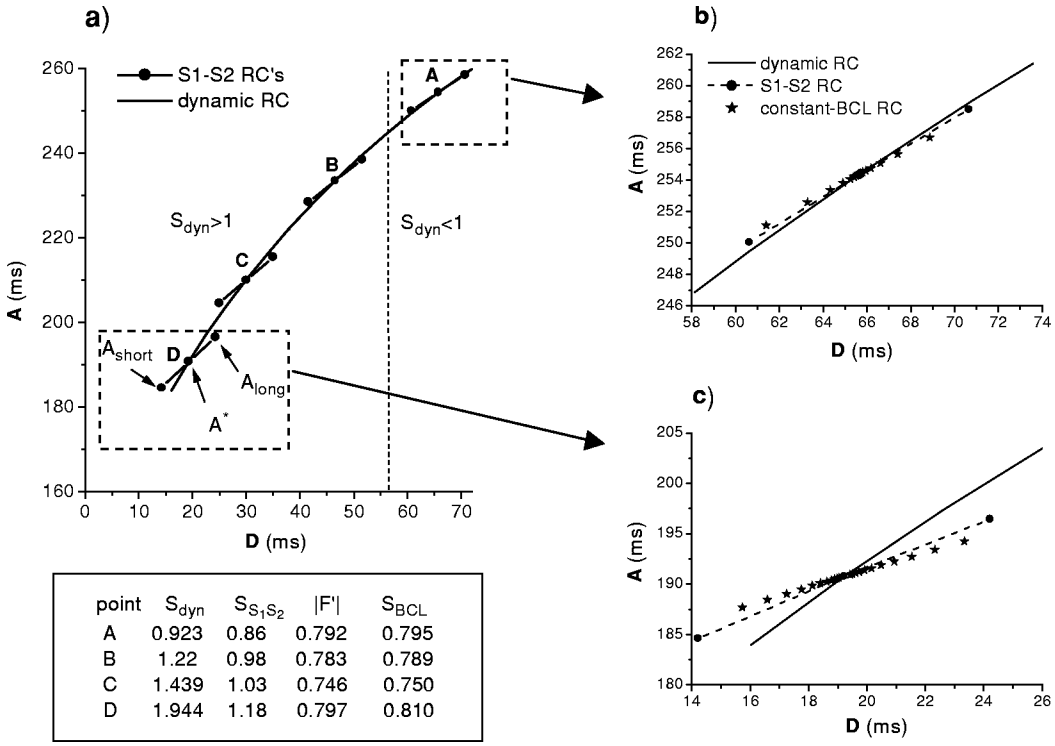

point	S_{dyn}	$S_{S_1S_2}$	$\lvert F'\rvert$	S_{BCL}
A	0.923	0.86	0.792	0.795
B	1.22	0.98	0.783	0.789
C	1.439	1.03	0.746	0.750
D	1.944	1.18	0.797	0.810

FIG. 6. Results of numerical simulation of the three-current ionic model illustrating the modified dynamic protocol. Parameter values from Table I were used, except $\tau_{sopen}=50$ ms. (a) The dynamic and local S1-S2 RCs, and values of their derivatives (S_{dyn}, $S_{S_1S_2}$, $|F'|$, and S_{BCL}) at several points. The estimated maximum error in determining $|F'|$ [according to Eq. (19)] is 0.5% and in determining S_{BCL} (using the linear least-squares fitting method) is 1%. The dashed vertical line indicates $S_{dyn}=1$. From the table, it is seen that $|F'|$ and $S_{\mathrm{BCL}}<1$ everywhere. The right panels show intersection of the constant BCL, dynamic, and S1-S2 RCs for points A (b) and D (c) in an expanded scale.

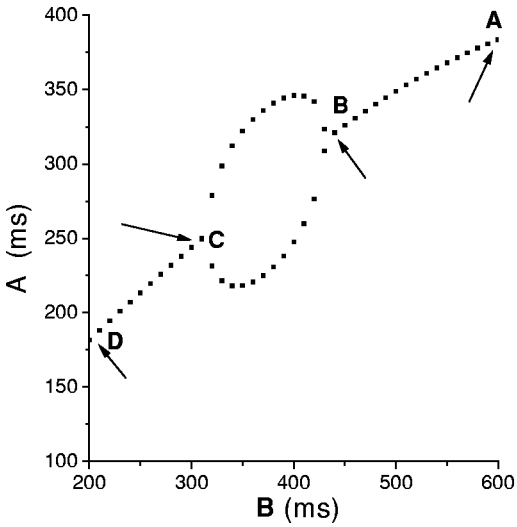

point	S_{dyn}	$S_{S_1S_2}$	$\|F'\|$	S_{BCL}
A	0.358	0.372	0.411	0.415
B	1.012	1.006	1.000	0.99
C	1.445	1.178	0.993	0.989
D	1.884	0.977	0.495	0.505

FIG. 7. Bifurcation diagram obtained from numerical simulations of the three-current ionic model with $\tau_{slow}=116$ ms and other parameters as in Table I. Arrows indicate fixed points, where values of the derivatives S_{dyn}, $S_{S_1S_2}$, $|F'|$, and S_{BCL} are determined, as given in the table. The estimated maximum error in determining $|F'|$ [according to Eq. (19)] is 0.5% and in determining S_{BCL} (using the linear least-squares fitting method) is 1%.

values of B, where steps 2 and 4 of the protocol were applied in order to obtain pairs (A_{long},D_{long}) and (A_{short},D_{short}). The table lists values of all slopes (S_{dyn}, $S_{S_1S_2}$, and $|F'|$) calculated in these points using formulas (19), (20), and (21). One can see that $|F'|$ is less than one in the entire region, indicating a stable 1:1 response, even when the slopes S_{dyn} and $S_{S_1S_2}$ become greater than one. The dashed vertical line correspond to the DI, where $S_{dyn}=1$. The right panel of Fig. 6 indicates the intersection of the constant BCL (obtained using step 3 of the protocol), dynamic, and S1-S2 RCs for points A and D in an expanded scale. We can see that for relatively slow pacing rate (point A) all these RCs are almost identical, whereas for faster pacing rate (point D) they differ from each other and have different slopes. The slope $|S_{\mathrm{BCL}}|$ of the constant-BCL RC at the intersection points calculated using linear least-squares fitting method is essentially equal to $|F'|$; a small difference is caused by a presence of the fast ionic current in the ODEs (this current was eliminated in order to derive a map) that becomes important at fast pacing rates.

Figure 7 shows the bifurcation diagram for a set of parameters that result in alternans (τ_{slow} changed to 116 ms). As seen in the graph, the transition from the 1:1 to the 2:2 response occurs at $B\simeq 440$ ms. As B decreases, the transition back to the 1:1 response takes place at $B\simeq 310$ ms. The figure also lists the slopes S_{dyn}, $S_{S_1S_2}$, $|F'|$, and S_{BCL}, evaluated at the transition points between 1:1 response and alternans and at other points away from the bifurcations. At very long B (point A) all slopes are much less than one. At $B\simeq 440$ ms (point B), where alternans first appears as B decreases, all slopes are very close to one. At $B\simeq 310$ ms (point C), where alternans returns to the 1:1 response, the slopes of the dynamic and S1-S2 RCs exceed one, while $|F'|$ and S_{BCL} are very close to one. At even smaller B (point D) S_{dyn} is much larger and $S_{S_1S_2}$ is a bit smaller than one, such that $|F'|$ is smaller than one.

Thus, the results of numerical simulations of the three-current model confirm that Nolasco and Dahlen's criterion fails to predict the existence of alternans in this model. A stable 1:1 response is observed even if the slopes of dynamic or S1-S2 RCs are much greater than unity. These results also show that the absolute value of the derivative F', either evaluated directly as S_{BCL}, or computed by combining S_{dyn} and $S_{S_1S_2}$ through Eq. (19), more accurately predicts the existence of alternans.

VII. DISCUSSION

This study presents a new stability criterion (19) for a one-dimensional mapping model of cardiac dynamics expressed in terms of easily obtainable experimental quantities. When tested on an example of a map derived from the three-current membrane model, criterion (19) is very accurate (see Figs. 5 and 6), while previously used criteria, which are based on the slope of the dynamic or S1-S2 RCs, fail to predict the stability of the 1:1 response pattern and transition to alternans.

The limitation of the stability criterion (19) is that it applies only when cardiac dynamics is adequately described by a map of form (6). This model limits the extent of cardiac memory to only one previous beat. If long-term memory effects are present, as indicated by some experimental studies [21] and described by some models [14], criterion (19) will fail in most cases. Thus, the pacing protocol described in Sec. IV and the stability criterion given by Eq. (19) can also be used to determine how well cardiac dynamics is described by map (5).

The advantage of the proposed stability criterion is that it can be easily used in actual experiments. The appropriate

procedure, described in Sec. IV, requires only a small modification of the existing dynamic protocol: the addition of two extra stimuli. However, one should keep in mind that this procedure will yield usable results only if the true steady state is reached at each pacing rate. This may require applying more stimuli at each pacing rate than it has been done in most studies, and may prolong the time it takes to collect the data. For example, one study in human hearts [9] suggests that the APD decays exponentially to the steady-state value with a time constant as long at 20 s so that pacing for as long at 1 min at each B may be needed to reach equilibrium. We also note that generalizations of the pacing protocol can be devised that use multipoint approximations to the derivative, determined by using multiple values of B_{short} and B_{long}. Nevertheless, this criterion provides a new tool for experimental the investigation of the dynamics of cardiac response during rapid pacing.

ACKNOWLEDGMENTS

We gratefully acknowledge the support of the National Science Foundation under Grant No. PHY-9982860. D.J.G. gratefully acknowledges the hospitality of the Aspen Center for Physics where fruitful discussions of this work with Professor Niels Otani and Professor Robert Gilmour, Jr., took place during the Workshop on Wave Dynamics in Biological Excitable Media.

APPENDIX: THE THREE-CURRENT IONIC MODEL

The three-current ionic model [16] contains three variables: the transmembrane potential v (scaled so that $v=0$ and $v=1$ are the rest and peak voltages, respectively), and two gating variables f and s (mnemonics: f is for fast, s is for slow). The voltage changes in response to the ionic currents according to the equation

$$\frac{dv}{dt} = -(J_{fast} + J_{slow} + J_{ung} + J_{stim}), \tag{A1}$$

and the currents J_{fast}, J_{slow}, and J_{ung} are simplified representations of sodium, calcium, and potassium currents, respectively.

The fast inward current J_{fast} has the form

$$J_{fast} = -fQ(v)/\tau_{fast}, \tag{A2}$$

where τ_{fast} is the time constant of this current, the voltage-dependent function $Q(v)$ is given by

$$Q(v) = \begin{cases} (v - V_{crit})(1-v) & \text{if } v > V_{crit} \\ 0 & \text{if } v < V_{crit}, \end{cases} \tag{A3}$$

and the gating variable f evolves according to the equation

$$\frac{df}{dt} = [f_\infty(v) - f]/\tau_f(v). \tag{A4}$$

Voltage-dependent functions f_∞ and τ_f are approximated by step functions

$$\begin{aligned} f_\infty(v) &= 0 \quad \text{and} \quad \tau_f(v) = \tau_{fclose} \quad \text{if} \quad v > V_{fgate} \\ f_\infty(v) &= 1 \quad \text{and} \quad \tau_f(v) = \tau_{fopen} \quad \text{if} \quad v < V_{fgate}. \end{aligned} \tag{A5}$$

Similarly, the slow inward current has the form

$$J_{slow} = -sS(v)/\tau_{slow}, \tag{A6}$$

where the sigmoid function $S(v)$ is given by

$$S(v) = \{1 + \tanh[\kappa(v - V_{sig})]\}/2, \tag{A7}$$

and the gating variable s is governed by the equations

$$\frac{ds}{dt} = [s_\infty(v) - s]/\tau_s(v), \tag{A8}$$

with s_∞ and τ_s given by

$$\begin{aligned} s_\infty(v) &= 0 \quad \text{and} \quad \tau_s(v) = \tau_{sclose} \quad \text{if} \quad v > V_{sgate} \\ s_\infty(v) &= 1 \quad \text{and} \quad \tau_s(v) = \tau_{sopen} \quad \text{if} \quad v < V_{sgate}. \end{aligned} \tag{A9}$$

The outward, ungated current has the form

$$J_{ung} = P(v)/\tau_{ung}, \tag{A10}$$

and its piecewise-linear voltage dependence is given by

$$P(v) = \begin{cases} 1 & \text{if} \quad v > V_{out} \\ v/V_{out} & \text{if} \quad v < V_{out}. \end{cases} \tag{A11}$$

The stimulus current J_{stim} is an external current applied by the experimenter. Typically, $J_{stim}(t)$ consists of a periodic train of brief pulses (the duration of 1 ms was used in our simulations), where the stimulus strength is set approximately to twice the amplitude required to excite fully recovered tissue. Table I lists the values of the parameters we used in our calculations unless otherwise stated.

[1] A. Karma, Chaos **4**, 461 (1994).

[2] M.A. Watanabe, N.F. Otani, and R.F. Gilmour, Jr., Circ. Res. **76**, 915 (1995).

[3] J.B. Nolasco and R.W. Dahlen, J. Appl. Physiol. **25**, 191 (1968).

[4] G.R. Mines, J. Physiol. (London) **48**, 349 (1913).

[5] M. Guevara, G. Ward, A. Shrier, and L. Glass, *Computers in Cardiology* (IEEE Computer Society, Silver Spring, MD, 1984), p. 167.

[6] R.F. Gilmour, N.F. Otani, and M.A. Watanabe, Am. J. Physiol. **272**, H1826 (1997).

[7] N.F. Otani and R.F. Gilmour, Jr., J. Theor. Biol. **187**, 409 (1997).

[8] M.R. Boyett and B.R. Jewell, J. Physiol. (London) **285**, 359

(1978).
[9] M.R. Franz, C.D. Swerdlow, L.B. Liem, and J. Schaefer, J. Clin. Invest. **82**, 972 (1988).
[10] V. Elharrar and B. Surawicz, Am. J. Physiol. **244**, H782 (1983).
[11] M.L. Koller, M.L. Riccio, and R.F. Gilmour, Jr., Am. J. Physiol. **275**, H1635 (1998).
[12] M.L. Riccio, M.L. Koller, and R.F. Gilmour, Jr., Circ. Res. **84**, 955 (1999).
[13] M.G. Hall, S. Bahar, and D.J. Gauthier, Phys. Rev. Lett. **82**, 2995 (1999).
[14] J.J. Fox, E. Bodenschatz, and R.F. Gilmour, Phys. Rev. Lett. **89**, 138101 (2002).
[15] E.G. Tolkacheva, D.G. Schaeffer, D.J. Gauthier, and C.C. Mitchell, Chaos **12**, 1034 (2002).
[16] F. Fenton and A. Karma, Chaos **8**, 20 (1998).
[17] S.H. Strogatz, *Nonlinear Dynamics and Chaos* (Perseus Books, Reading, MA, 1994), Chap. 10.
[18] W.H. Press, S.A. Teukolsky, W.T. Vetterling, B.P. Flannery, *Numerical Recipes in Fortran 77*, 2nd ed. (Cambridge University Press, Cambridge, 1999), Chap. 15.
[19] The central difference approximation for the derivative given by Eq. (21) cannot be used to calculate derivatives at the fixed points A_i^* at the bifurcation to alternans because the values of the fixed points inside the region of alternans are unknown. Instead, it is possible to estimate the derivative using a formula that takes into account the known fixed points lying to the other side of the fixed point A_i^* . The slope of the dynamic RC is then given by

$$S_{dyn} \approx \pm \frac{0.5A^*_{i\pm 2} - 2A^*_{i\pm 1} + 1.5A^*_i}{\Delta D},$$

where "+" "(−)" is used to determine derivative at the fixed point A_i^* lying after (before) the bifurcation to alternans. Here we assumed that the changes in the DI between two adjacent fixed points are equal, so that $\Delta D = |D_i^* - D_{i\pm 1}^*| = |D_{i\pm 1}^* - D_{i\pm 2}^*|$. This formula can be found, for example, in K.E. Atkinson, *An Introduction to Numerical Analysis*, 2nd ed. (Wiley, New York, 1989), p. 317.
[20] The derivative S_{dyn} can also be determining using a linear least-squares fitting method; see, for example, Ref. [18].
[21] M.A. Watanabe and M.L. Koller, Am. J. Physiol. **282**, H1534 (1983).